

A Comparison of AVIRIS and Landsat for Land Use Classification at the Urban Fringe

Rutherford V. Platt and Alexander F.H. Goetz

Abstract

In this study we tested whether AVIRIS data allowed for improved land use classification over synthetic Landsat ETM+ data for a location on the urban-rural fringe of Colorado. After processing the AVIRIS image and creating a synthetic Landsat image, we used standard classification and post-classification procedures to compare the data sources for land use mapping. We found that, for this location, AVIRIS holds modest, but real, advantages over Landsat for the classification of heterogeneous and vegetated land uses. Furthermore, this advantage comes almost entirely from the large number of sensor spectral bands rather than the high Signal-to-Noise Ratio (SNR).

Introduction

In rapidly urbanizing areas, such as the Front Range of Colorado, maps fast lose their validity. Large areas of prairie or farmland land can be overrun by residential development in a matter of months. Remotely sensed data allows land use and land cover to be mapped quickly, relatively cheaply, and frequently. With improved mapping of rapidly changing areas, planners will be able to better address issues associated with urban sprawl. However, the choice of sensor can significantly influence the accuracy of the classification. While it is commonly thought that smaller Ground Sampling Distance (GSD), also called pixel size, is the key to better land use classification, the number of spectral bands and the Signal-to-Noise Ratio (SNR) may influence classification accuracy as well.

Commonly, researchers use sensors such as those on Landsat or SPOT satellites for mapping land use and land cover (Table 1). Of these, the Landsat sensors have more spectral bands and a longer time series, while SPOT provides smaller GSD. Less traditional sensors may provide additional information that can improve mapping accuracy. The Airborne Visible Infrared Imaging Spectrometer (AVIRIS), for example, produces images with 224 spectral bands between 0.4 and 2.45 μm , compared to six bands for Landsat (not including the thermal band) and three for SPOT's Multispectral Imager (XS). Sensors with a large number of continuous spectral bands, such as AVIRIS, are called hyperspectral imagers (Green *et al.*, 1998).

Though hyperspectral imagers have been used in studies of mineralogical mapping and ecology, they have rarely been employed for land use mapping. A small number of studies have explored the integration of hyperspectral and Synthetic Aperture Radar (SAR) for urban mapping (Gamba and Housh-

mand, 2001; Hepner *et al.*, 1998). Other studies have used hyperspectral imagery to map a narrow range of urban materials and processes (Ben-Dor *et al.*, 2001; Ridd *et al.*, 1992; Salu, 1995). One study used an iterative spectral un-mixing procedure to delineate urban materials (Roessner *et al.*, 2001). To date, however, no studies have tested whether hyperspectral imagery improves land use classification accuracy over and above multispectral imagery such as from Landsat.

In this study, we tested whether AVIRIS data allowed for improved land use classification over synthetic Landsat ETM+ data for a location on the urban-rural fringe of Colorado. We expected that the large number of bands and high SNR provided by AVIRIS would help distinguish land cover types that are easily confused (irrigated urban areas and irrigated crops, for example). After processing the AVIRIS image and creating a synthetic Landsat image, we used standard classification and post-classification procedures to compare the data sources for land use mapping.

Sensor Specifications and Classification Accuracy: The Case of the Urban Fringe

Among the factors that may influence classification accuracy are the Ground Sampling Distance (GSD), number of spectral bands, and Signal-to-Noise Ratio (SNR) of a sensor. Generally, it is thought that GSD is the most important factor for classification accuracy of built environments (Forster, 1985). For example, a study in Indonesia found that SPOT Multispectral (XS) images are superior to Landsat Multispectral Scanner (MSS) images for mapping of heterogeneous, near-urban land cover because of SPOT's smaller pixel size (Gastellu-Etchegorry, 1990). The link between GSD and classification accuracy, however, is sometimes tenuous. In heterogeneous areas, such as residential areas, it has been shown that classification accuracies may actually improve by up to 20 percent as GSD is increased (Cushnie, 1987). This occurs when the reflectance spectra of a variety of cover types in an urban environment blend to form an overall urban signal that can be easily distinguished from other land covers.

SNR, which varies sensor-by-sensor and band-by-band and pixel-by-pixel, may also influence classification accuracy. The greater the SNR, the more usable information is available in the data. Overall, AVIRIS has much higher SNR than Landsat sensors. Within the Landsat family, the ETM+ in Landsat 7 has a higher SNR than the Thematic Mapper (TM) in Landsat 4 and 5. SNR may vary depending not only on sensor characteristics but also on the signal strength; summer images will have a higher SNR than winter images for the same time and place. While the advantages of high SNR are well documented in domains such as mineralogical mapping (Chabrilat *et al.*, 2002;

R.V. Platt was formerly with the Department of Geography, UCB 260, University of Colorado at Boulder, Boulder, CO 80309. He is presently with the Department of Environmental Studies, Gettysburg College, Gettysburg, PA 17325 (rplatt@gettysburg.edu).

A.F.H. Goetz is with the Center for the Study of Earth from Space/CIRES/Department of Geological Sciences, UCB 216, University of Colorado, Boulder, CO 80309 (goetz@cses.colorado.edu).

Photogrammetric Engineering & Remote Sensing
Vol. 70, No. 7, July 2004, pp. 813–819.

0099-1112/04/7007-0813/\$3.00/0
© 2004 American Society for Photogrammetry
and Remote Sensing

TABLE 1. SENSOR CHARACTERISTICS

	AVIRIS	Landsat TM/ETM+	SPOT XS
Platform	Airborne	Spaceborne	Spaceborne
Ground Sampling Distance	20 m	30 m	20 m
Number of Bands (excluding thermal)	224	6	3
Signal-to-Noise Ratio	High	Moderate	Moderate
Launch	1987	1982	1986

Smailbegovic *et al.*, 2000), they have not been thoroughly assessed for land use mapping. It is likely that the influence of SNR on classification accuracy depends heavily on the classes of interest. For example, distinguishing irrigated urban land from irrigated cropland may require a higher SNR than would be needed to distinguish spectrally disparate land uses such as residential land and fallow land.

Finally, the number of spectral bands may influence accuracy of land use classification. One study showed the benefits of increasing the number of bands in classification of the urban fringe. The study used SPOT XS data to map farmland and urban land uses in New Zealand (Gao and Skillcorn, 1998). In this case, using multispectral imagery improved the delineation of urban areas and farmland because vegetative land covers were easier to discriminate with a near-infrared

band. In cases where different land uses have similar but separable spectra, increasing the number of spectral bands will likely improve mapping accuracy. When land uses are either spectrally inseparable or clearly distinct, however, additional bands may not improve classification accuracy. In these cases the extra bands could add noise and spectral heterogeneity, resulting in lower classification accuracy.

These studies show that decreasing GDR, increasing SNR, and increasing the number of bands may improve classification accuracy for land use mapping, but the net benefits often depend on the particular scene and classification system. In this study AVIRIS data was compared with synthetic Landsat ETM+, fixed at 20 meter spatial resolution to determine the possible effects of increased number of bands and higher SNR for land use mapping at the urban fringe in Colorado.

Image Processing

An AVIRIS flight line was acquired for 30 September 1999 along the northern Front Range of Colorado. A single image cube was extracted that encompassed much of Fort Collins along with the surrounding agricultural land and Horsetooth Reservoir (Figure 1).

In order to convert at-sensor radiance into surface reflectance, an atmospheric correction was performed with High-Accuracy Atmosphere Correction for Hyperspectral Data (HATCH). Using spectral features within the data, HATCH creates pixel-by-pixel estimates of atmospheric composition. HATCH



Figure 1. Synthetic Landsat ETM+ Band 3 image of Fort Collins and surroundings.

takes advantage of recent advancements in atmospheric radiative transfer, resulting in highly accurate atmospheric corrections (Qu *et al.*, 2000; Qu *et al.*, 2002). After conducting the atmospheric correction, bands in the major water absorption features at 1.4 μm and 1.9 μm were removed.

In this study, an AVIRIS image was compared to synthetic Landsat ETM+ image derived from AVIRIS. This method eliminated several sources of error that would be present if a *real* Landsat image were used. First, AVIRIS images from 1999 and earlier contain unsystematic distortions introduced by the pitch, yaw, and roll of the aircraft (currently a three-axis gyroscope is attached to the sensor and records these movements so that the distortions may later be removed from the images). As a result, some AVIRIS images may be difficult to register to other images with high precision. Secondly, the GSD of AVIRIS (20 meters) is finer than that of Landsat (30 meters), necessitating a resampling procedure that would degrade and possibly introduce additional distortions to the image. Finally, the two images would be recorded at different times of the day, on different days, with different atmospheric conditions that would need to be corrected. Though it is likely that the cumulative effects of these differences would be small, they would no doubt introduce errors into the comparison.

A solution to all of these issues was to create an image from AVIRIS that closely matches the output of Landsat ETM+. This was done with a two-step process. In the first step, the appropriate AVIRIS bands were combined to approximate the following Landsat bands:

- Band 1: 0.45–0.52 μm (blue)
- Band 2: 0.52–0.60 μm (green)
- Band 3: 0.63–0.69 μm (red)
- Band 4: 0.76–0.90 μm (near infrared)
- Band 5: 1.55–1.75 μm (short wave infrared)
- Band 7: 2.08–2.35 μm (short wave infrared)

To create each synthetic ETM+ band, 7 to 27 AVIRIS bands were combined. Since each detector is most sensitive to the wavelength at the center of the sensor bandwidth, the AVIRIS bands that fell in the middle of a Landsat band were weighted more than those that fell toward the edge of the band, according to the Landsat ETM+ filter response function. Before proceeding, the dynamic range of the synthetic Landsat images was degraded from 12 bits to 8 bits to approximate ETM+.

In the second step, the SNR of the synthetic ETM+ image was degraded to approximate the SNR present in actual ETM+. In 1999, when the image was taken, AVIRIS bands had an SNR as high as approximately 1000 (figures from Robert O. Green, Jet Propulsion Laboratory, personal communication). Since noise is inversely proportional to the square root of the number of bands, the synthetic ETM+ has even lower noise than actual AVIRIS data and is approximately 28 to 37 times greater per band than that of ETM+ (Table 2). As a result, AVIRIS may outperform ETM+ even if spatial and spectral resolution were equalized.

TABLE 2. SIGNAL TO NOISE RATIO (SNR) OF SYNTHETIC AND TRUE LANDSAT ETM+

ETM+ Band	Average SNR for AVIRIS bands in synthetic ETM+	SNR of synthetic ETM+	Estimated SNR of true ETM+	Ratio of synthetic to true SNR
1	912	2412	87	28
2	1033	2923	96	31
3	982	2778	75	37
4	821	3178	147	22
5	584	2611	102	26
7	377	1958	67	29

To estimate the noise levels of ETM+, the following model was used (John Barker, NASA/Goddard Space Flight Center, personal communication):

$$\text{SNR} = \text{DN}/(a + b * \text{DN})^{.5}, \quad (1)$$

where *DN* is the digital number of a pixel, and *a* and *b* are coefficients for each band calibrated on ETM+ data from 06 September 2002. The model produced estimated per-pixel ETM+ SNR (scene averages shown in Table 2). Dividing the *DN*s by the estimated SNR produced an estimated noise level for each pixel. Gaussian noise images were then created with a standard deviation equal to this noise level (over and above that of AVIRIS) for each pixel of each band. These noise images were added to each synthetic ETM+ band to approximate the noise in the actual ETM+ sensors. The resulting synthetic ETM+ images very closely approximated the bands and SNR of actual Landsat ETM+, only with a GSD of 20 meters instead of 30 meters.

After creating the synthetic Landsat image, a Maximum Noise Fraction (MNF) transform was performed on the AVIRIS cube and synthetic Landsat images to reduce processing time and noise, (Green *et al.*, 1988. Note: MNF is referred to as “Minimum Noise Fraction” in Environment for Visualizing Images (ENVI) image processing software). A MNF transform, similar to a principal components transform, derives a series of uncorrelated bands and segregates noise in the data. Unlike a principal components transform, a MNF transform equalizes the noise across bands so that image data with variance lower than noise is not hidden in higher bands. All MNF bands with an eigenvalue of less than two were eliminated since these bands contain mostly noise. The number of remaining bands equals the dimensionality of the image. In this case, the synthetic ETM+ data had a dimensionality of five, and the AVIRIS data had a dimensionality of 30. All subsequent analysis was conducted on these two data sets.

Figures 2 and 3 show the band loadings for MNF bands 1 to 5 and 16 to 30. There are 210 AVIRIS bands between 0.4 and 2.5 μm . The first few MNF bands (Figure 2) show loadings that peak in the atmospheric windows and are not single-wavelength specific. In fact, the peak loadings fall approximately in line with the Landsat bands. On the other hand, in the higher MNF bands (Figure 3) the loadings are much more wavelength specific as evidenced by the sharp changes throughout the spectrum. Some of these significant loadings are associated

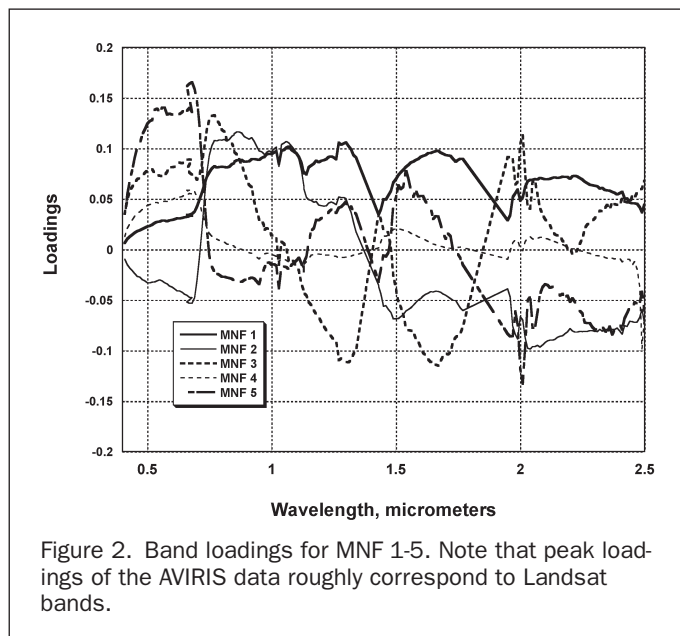
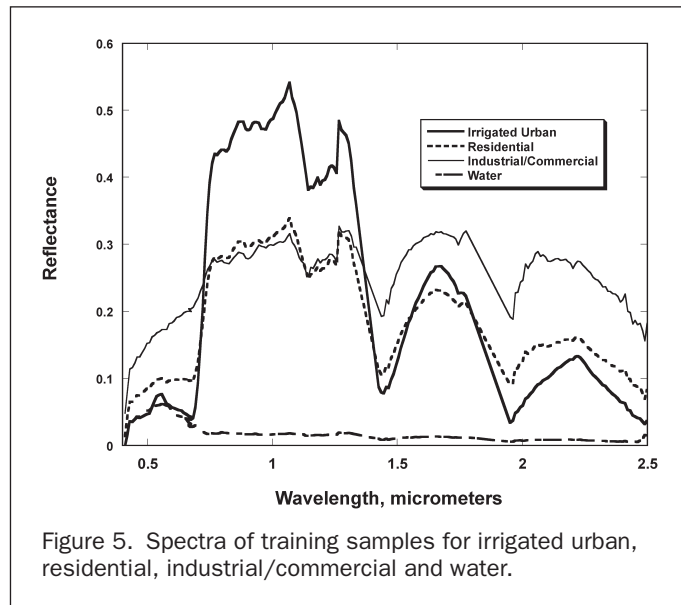
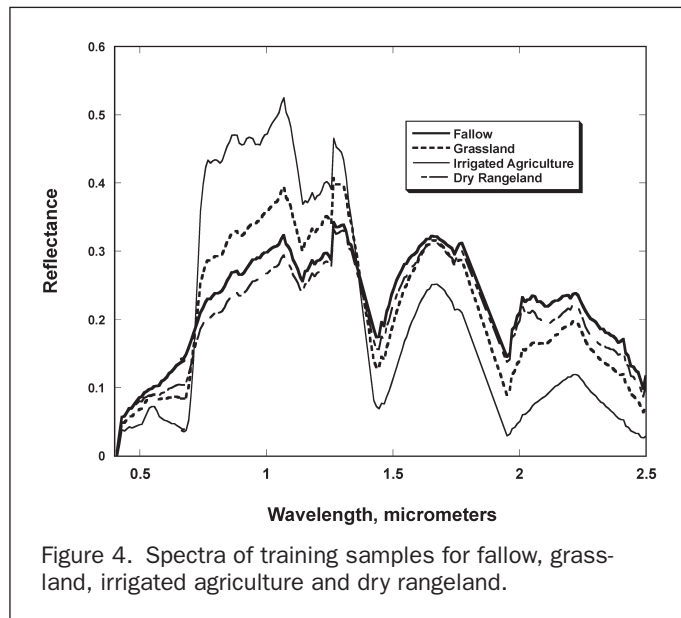
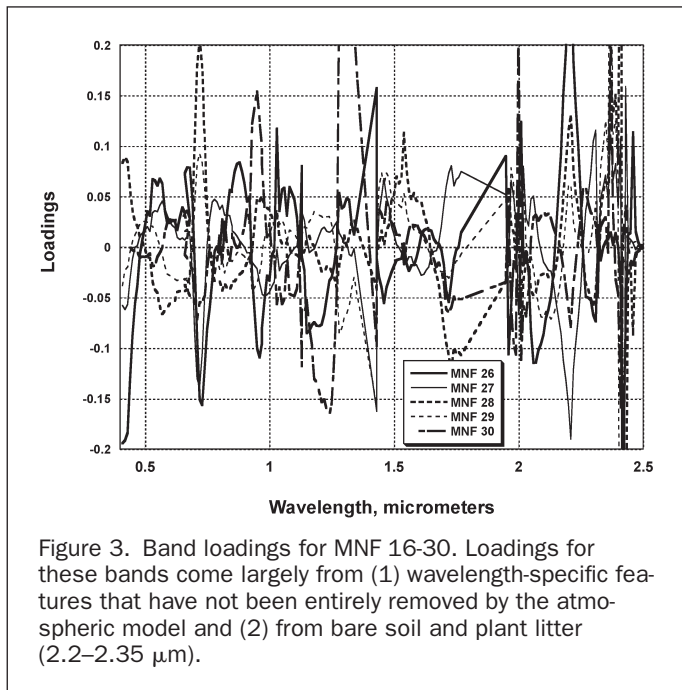


Figure 2. Band loadings for MNF 1-5. Note that peak loadings of the AVIRIS data roughly correspond to Landsat bands.



with the water vapor absorption bands at 0.94 and 1.14 μm , and the CO_2 features around 2.1 μm . These features are not completely removed by the atmospheric model, and hence induce low-amplitude variability in the data that is manifested in the statistics of the image. Loadings around 2.2 to 2.35 μm are most likely associated with bare soil and plant litter.

Classification Methodology

There are myriad classification methods, each with different properties. Unsupervised classification automatically separates land use into a number of computer-defined categories. Supervised classification assigns each pixel to a class by matching its spectrum to that of a defined class. Linear spectral mixing derives pixel-by-pixel measures of abundance for spectrally pure materials.

This study used a variety of supervised classification algorithms but focused on a single one: the Maximum Likelihood (ML) classifier. ML is a widely accepted classification method because of its robustness and simplicity. The classifier determines the probability that a pixel belongs to each class and then assigns the pixel to the class with the highest probability (Richards, 1999). It assumes that the spectrum of each class is normally distributed and requires that the class be defined by a minimum $n + 1$ training pixels for n spectral bands.

Using ENVI, images were classified into eight classes with the ML classifier. The classification system was a modification of Anderson Level II (Anderson *et al.*, 1976) and used training samples from the following land use categories: residential, commercial/industrial, water, irrigated cropland, fallow, dry rangeland, grassland, and irrigated urban. Training samples with a minimum of 300 pixels were defined using the interiors of relatively homogenous features in each land use class. The spectra of these training samples (also called ROIs or Regions Of Interest) show that these land use classes are, on average, spectrally separable (Figures 4 and 5). Many, however, have some characteristics of vegetation since all land use classes contain some vegetation.

To assess classification accuracy, the supervised classifications were then compared to a ground truth image. The ground

truth image was created with a hand classification of a USGS Digital Orthophoto Quarter Quad (DOQQ) taken on 04 October 1999, five days after the AVIRIS flight. Site visits, information from the National Land Cover Data set (NLCD) (Vogelmann *et al.*, 1998), and several bands of the AVIRIS data itself were used in the hand classification process when the land use was not clear from the DOQQ alone. The ground truth image was geometrically registered to the AVIRIS image using a 1-degree polynomial and bilinear resampling with 20 ground control points. The rectification had a RMSE of 0.45.

Results

Accuracy of a supervised classification of land use typically ranges between 60 percent–90 percent depending on the classification scheme, the classifier, and the image itself. Ancillary data, textural data, or post-classification rules may further increase the classification accuracy. These were not used in this study, however, since the goal was not to maximize classification accuracy, but to compare the performance of different

image types with a commonly accepted classification procedure.

Visually, the two classifications produced similar results, though the AVIRIS classification appears to have smoother edges and fewer isolated pixels. The accuracy assessment verified that the AVIRIS classification was superior to that of the synthetic ETM+ image. This remained true with all four classifiers tested, though classification accuracy varied widely. Importantly, the results of the synthetic ETM+ classification were virtually identical to a similar classification of ETM+ without added noise. This indicates that the difference in noise between AVIRIS and ETM+ is not enough to strongly influence classification accuracy in this scene. Henceforth, only results for synthetic ETM+ with added noise will be reported.

The ML classifier produced the highest classification accuracies for both AVIRIS and synthetic Landsat, and the difference between the two was the smallest (Table 3). Using ML, classification of AVIRIS improved 5 percent over synthetic Landsat, while the Kappa coefficient (which compensates for correct classification by chance) increased from .59 to .65. A pair-wise comparison of the kappa statistics (Rogan *et al.*, 2002; Congalton and Green, 1998) for the two classifications shows that these results are significantly different from each other with a z-value of 78.32. A z-value of 1.96 or higher indicates that two kappa values are significantly different at the 95 percent confidence level.

TABLE 3. ACCURACY OF SUPERVISED CLASSIFICATION WITH COMMON CLASSIFIERS

	AVIRIS		Synthetic ETM+		Difference	
	Accuracy	Kappa	Accuracy	Kappa	Accuracy	Kappa
Parallelepiped	35	0.25	30	0.19	5	0.06
Minimum Distance	72	0.64	64	0.54	8	0.10
Mahalanobis Distance	69	0.61	53	0.43	17	0.18
Maximum Likelihood	73	0.65	68	0.59	5	0.06

Accuracy assessment at the class level was conducted with an unstratified random sample of 28,058 pixels (10 percent of the image). It showed that changes in classification accuracy varied widely between classes (Table 4). Producer's accuracy measures the chance that a pixel is classified as x given that the ground truth indicates that it is x. It is sensitive to errors of omission. User's accuracy describes the chance that the ground truth image indicates that it is x given that it has been classified as x. It is sensitive to errors of commission.

Using the AVIRIS image, the producer accuracy improved in five of eight classes but decreased for the other three. Builtup areas (residential and commercial/industrial) both improved by 11 percentage points, while urban irrigated areas improved by seven. At the same time, the classification accuracy of fallow decreased by 11 and dry rangeland decreased by five. For these land covers, the classification using AVIRIS failed more often to identify the classes. Because a large portion of the image is composed of the classes that improved, however, AVIRIS led to an improvement in overall classification accuracy.

User's accuracy benefited much more from AVIRIS than did producer's accuracy. Of the eight classes, four strongly benefited from AVIRIS; fallow improved by 58 percentage points, while irrigated improved by 37, dry rangeland by 18 and urban irrigation by 17. Only commercial/industrial substantially decreased (-9 percent) in user's accuracy using AVIRIS. This indicated that there were fewer false positives from these vegetation and soil-based classes but more false positives for commercial areas.

The change in the confusion matrix reveals important details of the different classification accuracy of AVIRIS and synthetic ETM+ (Table 5). Along the diagonal, numbers indicate the change in classification accuracy by class for AVIRIS over synthetic Landsat. On the off-diagonal, numbers show the change in misclassification; a negative number indicates that the classification does not confuse these classes as often with AVIRIS data. Reading from top to bottom, one can assess where classification accuracy increased and where it decreased using AVIRIS data. Overall, AVIRIS data improved the ability to distinguish several easily confused classes including residential

TABLE 4. ACCURACY OF MAXIMUM LIKELIHOOD CLASSIFICATION BY CLASS

	Sample Size	Producer Accuracy			User Accuracy		
		AVIRIS	ETM+	Change	AVIRIS	ETM+	Change
Residential	10032	82	71	11	74	75	-1
Dry Rangeland	4831	71	75	-5	92	75	18
Irrigated Urban	744	63	56	7	49	33	17
Fallow	624	66	77	-11	87	29	58
Grassland	6384	59	55	4	70	65	5
Com/Industrial	3115	71	60	11	49	59	-9
Water	2108	87	91	-4	100	99	0
Irrigated Cropland	221	72	68	4	73	36	37

TABLE 5. CHANGE IN CLASSIFICATION ACCURACY BY CLASS (AVIRIS OVER SYNTHETIC ETM+)

Synthetic ETM+→ AVIRIS ↓	Residential	Dry Rangeland	Urban Irrigation	Fallow	Grassland	Com/ Indust	Water	Irrigated Crops
Residential	11	0	6	2	10	-3	-3	7
Dry Rangeland	-3	-5	-1	-3	-8	-4	-1	-1
Urban Irrigation	-2	0	7	0	-2	0	1	-6
Fallow	-2	-7	-1	-11	-7	-4	0	0
Grassland	-4	3	-5	1	4	0	0	-4
Com/Industrial	0	9	2	11	5	11	8	1
Water	0	0	0	0	0	0	-4	0
Irrigated Crops	-1	0	-8	0	-1	0	0	4

versus vegetated land uses; commercial/industrial versus fallow, dry rangeland, and residential; and, urban irrigation versus irrigated crops and grassland.

The net improvement did not take place in all categories, however. Using AVIRIS, the classification accuracy of fallow decreased due to increased confusion with commercial/industrial. Dry rangeland was also more likely to be confused with commercial/industrial, though less likely to be confused with fallow.

Discussion

The classified images contained similar types of misclassifications, often due to the well-identified problem of heterogeneity in urban land covers (Forster, 1985). Residential areas were sometimes confused with vegetated land uses because both have mixtures of soil and vegetation. Similarly, commercial/industrial areas were sometimes confused with fallow and dry rangeland because all of these land uses may contain highly reflective exposed ground. Water was misclassified in places because differences in chlorophyll content, depth and turbidity sometimes gives it similar spectral characteristics to other classes. Urban irrigation was confused with irrigated crops and grassland because all have leafy plants high in chlorophyll that reflect strongly in the infrared. Since there are often many-to-one or one-to-many relationships between a spectrum and land use, these errors are common under almost any classification system or sensor. However, beneath the similarities, there were important differences between the classifications.

Overall, the results support the hypothesis that AVIRIS data contained information over and above synthetic Landsat that helped to improve classification accuracy for land use in this scene. This additional information may have come from areas of the spectrum captured only by AVIRIS (e.g., .90 to 1.35 μm , 1.43 to 1.55 μm , and 1.95 to 2.08 μm). For example, a graph of mean spectra for land use training samples shows that the region around 1.17 μm helps to identify urban irrigation and the region around 1.45 μm helps to distinguish residential areas from industrial/commercial areas (Figures 4 and 5). The additional information could also have come from the high spectral resolution of AVIRIS; each synthetic Landsat band is composed of a weighted average of at least seven AVIRIS bands.

In terms of producer's accuracy, this improvement appeared to be most pronounced in land use classes with a large amount of vegetation such as residential land, urban irrigation, grassland, and irrigated agriculture. The improvement in these classes most likely occurred because the signal of vegetation (part of the mix for all these classes) contained some distinction that only AVIRIS could pick up. This could be a distinct vegetation type, moisture content, stress level or other spectral characteristic that set a given land use apart from another land use. In addition, improvements in producer's accuracy tended to be in spectrally heterogeneous classes such as residential and commercial/industrial. Perhaps the classification of the AVIRIS image was able to detect the full range of spectral features that appeared in these classes. In addition to changes in producer's accuracy, the user's accuracy improved across most classes. The false positives decreased, in some cases dramatically, again perhaps because subtle signatures in the spectrum distinguished easily confused classes.

The decrease in accuracy for certain classes is more difficult to explain. For example, the producer's accuracy for fallow, water, and dry rangeland decreased with AVIRIS. In these fairly homogenous land uses, perhaps the additional bands in AVIRIS simply added noise and provided no additional useful information over synthetic Landsat. The decrease in user's accuracy for commercial and industrial land is also difficult to explain. It is possible that certain spectral similarities between fallow and commercial/industrial are not evident in the

wavelengths covered by the six synthetic Landsat bands. In these cases, spurious similarities between the land uses would only be detected by AVIRIS.

Conclusion

In this study, a supervised classification of AVIRIS was more accurate than one of synthetic Landsat ETM+ for land use classification at the urban fringe. Which imagery a researcher should use, provided both are available, largely depends on the purpose of the study. If the goal is to accurately identify existing built and highly vegetated land covers (important for mapping sprawl, for example) AVIRIS holds an apparent advantage. If the objective is to minimize false positives for land uses with a mix of soil and vegetation, AVIRIS again holds an advantage. On the other hand, using AVIRIS produced a greater number of false positives for commercial/industrial land and performed poorly in classifications of relatively homogenous, less-vegetated land uses, such as fallow and dry rangeland. If these are the classes of greatest interest, perhaps Landsat should be used.

Since classification accuracy is dependent on a number of factors besides sensor specifications, caution should be used in extending the conclusions of this study to other areas. For example, using other classification systems such as the Food and Agriculture Organization's Land Cover Classification system (LCCS) or the V-I-S system may yield different classification accuracies for the two sensors (see Di Gregorio, 2000 and Ridd, 1995 for a description of these classification systems). Furthermore, these results may not hold for a different mix of land covers.

A final finding of this study is that the overall advantage of AVIRIS came not from its high SNR, but from the number of spectral bands. This suggests that future satellites used for land use mapping should include a sensor with a larger number of spectral bands in the 0.4 to 2.5 μm region. However, this satellite need not have higher SNR than Landsat ETM+ for accurate land use classification at the urban fringe.

Acknowledgments

Funding from the EPA STAR program (Grant U915889-01-1) made this project possible. Thanks to the International Institute of Applied Systems Analysis (IIASA) for supporting the latter stage of the project and to Ethan Gutmann who assisted with IDL. Finally, thanks to the persistent reviewer who helped make this a better manuscript.

References

- Anderson, J.R., E. Hardy, J. Roach, and R. Witmer, 1976. *A Land Use and Land Cover Classification System for Use with Remote Sensor Data*, U.S. Geological Survey Professional Paper 964.
- Ben-Dor, E., N. Levin, H. Saaroni, 2001. A spectral based recognition of the urban environment using the visible and near-infrared spectral region (0.4–1.1 μm). A case study over Tel-Aviv, Israel, *International Journal of Remote Sensing*, 22(11):2193–2218.
- Chabrilat, S., A.F.H. Goetz, L. Krosley, and H.W. Olson, 2002. Use of hyperspectral images in the identification and mapping of expansive clay soils and the role of spatial resolution, *Remote Sensing of Environment*, 82:431–445.
- Congalton, R.G., and K. Green, 1998. *Assessing the Accuracy of Remotely Sensed Data: Principles and Practices*, Lewis Publishers, Boca Raton, Florida, pp. 50–51.
- Cushnie, J.L., 1987. The Interactive Effect of Spatial Resolution and Degree of Internal Variability within Land-Cover Types on Classification Accuracies, *Photogrammetric Engineering & Remote Sensing*, 8(1):15–29.
- Di Gregorio, A., and L.J.M., Jansen, 2000. *Land Cover Classification System (LCCS) Classification Concepts and User Manual*, Food and Agriculture Organization of the United Nations, Rome.

- Forster, B.C., 1985. An examination of some problems and solutions in monitoring urban areas from satellite platforms, *International Journal of Remote Sensing* 6(1):139–151.
- Gamba, P., and B. Houshmand, 2001. Integration of hyperspectral and IFSAR data for improved 3D urban profile reconstruction, *Photogrammetric Engineering & Remote Sensing*, 67:947–956.
- Gao, J., and D. Skillcorn, 1998. Capability of SPOT XS Data in Producing Detailed Land Cover Maps at the Urban-Rural Periphery, *International Journal of Remote Sensing* 19(15):2877–2891.
- Gastellu-Etchegorry, J.P., 1990. An Assessment of SPOT XS and Landsat MSS Data for Digital Classification of Near-Urban Land Cover, *International Journal of Remote Sensing*, 11(2):225–235.
- Green, A.A., M. Berman, P. Switzer, and M.D. Craig, 1988. A transformation for ordering multispectral data in terms of image quality with implications for noise removal, *IEEE Transactions on Geoscience and Remote Sensing*, 26(1):65–74.
- Green, R.O., M.L. Eastwood, C.M. Sartare, T.G. Chrien, M. Aronsson, B.J. Chippendale, J.A. Faust, B.E. Pavri, C.J. Chovit, M.S. Solis, M.R. Olah, and O. Williams, 1998. Imaging spectroscopy and the Airborne Visible Infrared Imaging Spectrometer (AVIRIS), *Remote Sensing of Environment*, 65:227–248.
- Hepner, G.F., B. Houshmand, I. Kulikov, and N. Bryant, 1998. Investigation of the integration of AVIRIS and IFSAR for urban analysis, *Photogrammetric Engineering & Remote Sensing*, 64:813–820.
- Qu, Z., Goetz, A.F.H., Heidebrecht, K.B., 2000. High-Accuracy Atmosphere Correction for Hyperspectral Data (HATCH), *Proceedings of the Airborne Visible/Infrared Imaging Spectrometer (AVIRIS) 2000 Workshop*. Jet Propulsion Laboratories Publication 00–18.
- Qu, Z., B.C. Kindel, and A.F.H. Goetz, 2002. The High-Accuracy Atmospheric Correction for Hyperspectral Data (HATCH) Model, *IEEE Transactions on Geoscience and Remote Sensing*, in press.
- Richards, J.A., 1999. *Remote Sensing Digital Image Analysis*, Springer Verlag, New York.
- Ridd, M.K., 1995. Exploring a V-I-S (Vegetation-Impervious Surface-Soil) Model for Urban Ecosystem Analysis through Remote Sensing: Comparative Anatomy for Cities, *International Journal of Remote Sensing*, 16(12):2165–2185.
- Ridd, M.K., N.D. Ritter, N.A. Bryant, and R.O. Green, 1992. AVIRIS data and neural networks applied to an urban ecosystem, *3rd Annual JPL Airborne Geoscience Workshop*, Pasadena, California.
- Roessner, S., K. Segl, U. Heiden, and H. Kaufmann, 2001. Automated differentiation of urban surfaces based on airborne hyperspectral imagery, *IEEE Transactions on Geoscience and Remote Sensing*, 39:1525–1532.
- Rogan, J., J. Franklin, and D.A. Roberts, 2002. A comparison of methods for monitoring multitemporal vegetation change using Thematic Mapper imagery, *Remote Sensing of Environment*, 80: 143–156.
- Salu, Y., 1995. Sub pixel localization of highways in AVIRIS images, *5th Annual JPL Airborne Geoscience Workshop*, Pasadena, CA.
- Smailbegovic, A., J.V. Taranik, and F. Kruse, 2000. Importance of Spatial and Radiometric Resolution of AVIRIS Data for Recognition of Mineral Endmembers in the Geiger Grade Area, Nevada, U.S.A., *Proceedings of the Airborne Visible/Infrared Imaging Spectrometer (AVIRIS) 2000 Workshop*, Jet Propulsion Laboratories Publication 00–18.
- Vogelmann, J.E., T. Sohl, and S.M. Howard, 1998. Regional characterization of land cover using multiple sources of data, *Photogrammetric Engineering & Remote Sensing*, 64:45–57.

(Accepted 28 May 2003; revised 26 July 2003)